

Structure of Aqueous Sodium Aluminate Solutions: A Solution X-ray Diffraction Study

Tamás Radnai*

Central Research Institute for Chemistry, Hungarian Academy of Sciences, Budapest, Hungary

Peter M. May, Glenn T. Hefter, and Pál Sipos

Department of Chemistry, Murdoch University, WA 6150, Australia

Received: February 23, 1998; In Final Form: July 6, 1998

A structural analysis of six alkaline sodium aluminate aqueous solutions by the X-ray diffraction method is reported. On average, each Al atom is surrounded by four oxygens, indicative of the predominance of $\text{Al}(\text{OH})_4^-$ (aq) in these solutions. Detailed least-squares fitting indicates that a significant contraction of the Al–O distances occurs with increasing aluminate concentration, from 1.80 Å at 2 M to 1.74 Å at 6 M $\text{Al}(\text{OH})_3$ in 8 M NaOH. The local structure has been described by models that have separate hydrated ions in the most dilute aluminate solution but contact sodium aluminate ion pairs in the most concentrated solution. The hydration number of the sodium ion decreases with increasing concentration, but the overall coordination number appears to be unchanged by the ion pair formation. An extensive rearrangement in the hydrogen-bonded network of bulk water also occurs as the aluminum concentration rises, with the appearance of new diffraction distances at 3.3 and 3.9 Å. A gradual appearance and disappearance of shorter hydrogen bonds between first neighboring O atoms is observed. The data are consistent with the occurrence of oligomeric aluminate species but are not conclusive within the limits of the experimental error.

Introduction

Sodium aluminate solutions have been intensively investigated, by various physicochemical techniques over the last two decades.

Alkaline aluminate liquors are important because of their use in the extraction of alumina from bauxite.¹ However, the chemical characterization of these solutions is difficult because they are chemically aggressive and, like all highly concentrated electrolyte solutions, hard to deal with both theoretically and experimentally. Indeed, many of the most powerful analytical techniques for studying chemical speciation in solution such as potentiometry^{2–6} and NMR,^{7–13} UV–Vis,^{12–15} and IR/Raman^{9,12,16–19} spectroscopies have had limited success in providing useful information about these solutions, as evidenced by a striking lack of agreement between them.²⁰

Although some solution X-ray diffraction measurements were made as part of a much larger study of alkaline aluminate solutions in Hungary in the 1970s,²¹ no structural conclusions were drawn and the data have not been published in the open literature. The present paper reports a systematic structural investigation by solution X-ray diffraction of a wide concentration range of pure aqueous alkaline aluminate solutions. The key advantage of this technique from the chemical speciation standpoint is that, unlike other probes, its results are little affected by the nonspecific (i.e., nonbonding) solute–solute interactions which predominate in concentrated electrolyte solutions.

Experimental

Materials and Solutions. Concentrated NaOH stock solutions (ca. 20 M) were prepared from analytical grade NaOH

(98 w/w%, Ajax Chemicals, Australia) and Millipore MilliQ water.²² After standing for 2–3 days, the stock solution was filtered through a supported membrane (0.45 μm pore size) equipped with a CO₂ trap to remove solid Na₂CO₃ which is salted out almost quantitatively. Analysis by high-precision pH titrimetry²³ indicated carbonate concentrations less than 0.05% of the total alkalinity (i.e., <10 mM). More dilute NaOH solutions were prepared from the stock solutions by weight (without buoyancy correction).

Sodium aluminate solutions were prepared by quantitative dissolution of degreased Al wire (Goodfellow, U.K., “99.999%” grade) as described elsewhere.²² All the aluminate solutions contained 10 ppm sodium gluconate (Sigma-Aldrich, “99%” grade) as a seed-poison which was added to the solutions prior to dissolving the aluminum metal. After dissolution, the solutions were filtered (0.45 μm) and stored in sealed Pyrex-glass containers at room temperature. No visible precipitation occurred in these solutions, even after storage for as long as 3 months, and analysis indicated no silica contamination.

To calculate the exact concentrations (mol dm⁻³, M) of NaOH and Al(III) in the resulting solutions, densities were measured either using an Anton Paar DMA 02D high-precision density meter (using air and distilled water as density standards) or pycnometrically at 25.0 ± 0.02 °C.

Chemical compositions and densities of each sodium aluminate solution and the two reference liquids, pure water and 8 M NaOH solution, are given in Table 1. It should be noted that two solutions (*n*83 and *n*85) were prepared and measured independently from the rest of the series. The solutions (with the exception of solution *n*86, see below) were prepared in Australia and couriered immediately to Hungary for the measurements, some 2–10 weeks later. The most supersaturated solution (*n*86) was prepared in Hungary immediately

* Author to whom correspondence should be addressed at Central Research Institute for Chemistry, Hungarian Academy of Sciences, Budapest, P.O. Box 17, H-1525, Hungary.

TABLE 1: Composition and Densities of the Sodium Aluminate and Reference Solutions^a

	code of solution							
	water	<i>n</i> 21	<i>n</i> 8	<i>n</i> 82	<i>n</i> 83	<i>n</i> 84	<i>n</i> 85	<i>n</i> 86
salt concn mol no.								
NaOH	0	2.707	7.771	7.830	8.205	7.938	8.206	8.625
Al(OH) ₃	0	1.114	0	1.976	2.663	3.995	5.152	6.358
Na ⁺	0	2.707	7.771	7.830	8.206	7.938	8.206	8.625
Al	0	1.114	0	1.976	2.663	3.995	5.152	6.358
OH ⁻	0	6.048	7.771	13.76	16.19	19.92	23.66	27.69
H ₂ O	55.51	52.33	53.09	47.54	45.94	42.21	38.95	35.83
total	55.51	62.19	68.64	71.11	73.01	74.07	75.97	78.51
density (<i>d</i>)	1.000	1.138	1.267	1.324	1.366	1.389	1.432	1.486
number (ρ_0)	0.0334	0.0374	0.0413	0.0428	0.0439	0.0446	0.0457	0.0473

^a The salt concentrations are in mol dm⁻³, the number of moles of scattering units refer to 1 dm³ of solution, macroscopic mass densities (*d*) are in kg dm⁻³, and number densities of "scattering units" (ρ_0) in 10²⁴ cm⁻³ units.

before the X-ray diffraction experiment; visible signs of precipitation were observed ca. 1 month after preparation of this solution.

There are many reports in the literature indicating that the hydrolysis of Al(III) can be slow; however, such reactions are not relevant to the highly alkaline conditions dealt with in this work under which none of the early stepwise hydroxy complexes [Al(OH)₂²⁺, Al(OH)₂⁺, and possibly Al(OH)₃] remain stable. On the contrary, considerable evidence has been accumulated by the present authors demonstrating that, provided no precipitation of Al(OH)₃(s) occurs, kinetic effects are not exhibited by these synthetic Bayer liquors over the time scale of our measurements (i.e., for any observation taking longer than about a minute).

X-ray Diffraction Measurements. X-ray diffraction measurements were performed in a thermostated room at a temperature of 25 ± 1 °C on a θ - θ type diffractometer, made by Seifert & Co., using MoK α radiation with a wavelength of 0.711 Å. The observed range of scattering angles (2 θ) was between ca. 1.5° and 110°. The scattered intensity was recorded as 155 data points, equally spaced over the range of scattering angles and each counted over a 6 min sampling period. This gave a total of 40 000 to 240 000 counts per point. The method of measurement and data treatment were as previously reported,²⁴ including corrections for background, polarization, absorption, subtraction of the scattering pattern of the empty cell, and conversion of the corrected intensities into absolute units.

Special care was taken over the material used for the sample holder. Since the samples were of extremely high purity and strongly alkaline, some of them supersaturated, the material of the polymer windows of the cell was of great importance. After a series of preliminary experiments using a variety of polymer films with amorphous X-ray scattering patterns, ca. 75 μ m thin foils of bi-oriented polypropylene were selected as the most suitable. These appeared fully resistant to the alkaline solutions and produced little background scattering.

The experimental structure function $kH(k)$ is defined as

$$kH(k) = k[I_{\text{abs}}(k) - \sum_{\alpha} x_{\alpha} f_{\alpha}^2(k) - \sum_{\alpha} x_{\alpha} I_{\alpha, \text{inc}}(k)]M(k) \quad (1)$$

where k is the scattering variable, $k = 4\pi/\lambda \sin(\theta)$, λ the wavelength of incident radiation, $I_{\text{abs}}(k)$ the corrected intensity converted to absolute units, x_{α} the mole fraction, $f_{\alpha}(k)$ the coherent scattering factor, and $I_{\alpha, \text{inc}}(k)$ the incoherent scattering of an α type scattering unit. $M(k)$ is the modification function

$$M(k) = \frac{\exp(-bk^2)}{[\sum_{\alpha} x_{\alpha} f_{\alpha}(k)]^2} \quad (2)$$

where the sum is extended over each type of X-ray scattering unit in the sample solution. The value of b is arbitrary, selected as $b = 0.003$. Four types of scattering units were considered as being present in the solutions: Na⁺ and OH⁻ ions, H₂O molecules, and Al atoms. The arbitrary use of a composite "group" scattering unit, representing both OH⁻ and H₂O instead of individual O and H atoms, proved to be useful for the description of the X-ray scattering of the many H-containing molecules and ions. This is necessary because of the low sensitivity of X-rays in the detection of separate H atoms. Accordingly, throughout this paper, whenever a scattering unit is denoted O, it refers to the composite scattering of both OH⁻ and H₂O.

All necessary scattering factors and incoherent intensity contributions were computed as analytical expressions. The parameters required to compute the scattering factors were taken from the literature²⁵ for all scattering units, except for OH⁻ which were taken from Narten.²⁶ The incoherent intensities were calculated according to Pálinkás and Radnai for O, H, Na, and Al²⁷ and according to Hajdu for H₂O.²⁸

The experimental pair distribution functions $g(r)$ were computed from the structure functions according to

$$g(r) = 1 + \frac{1}{2\pi^2 \rho_0} \int_{k_{\min}}^{k_{\max}} k^2 H(k) j_0(kr) dk \quad (3)$$

where r is the interatomic distance, k_{\min} and k_{\max} are the lower and upper limits of the range of experimental data, ρ_0 is the bulk number density of the X-ray scattering units, and j_0 is the 0th order spherical Bessel function.

Results

Experimental Structure Functions. The experimental structure functions are shown in Figure 1. Although these exhibit visible differences across the series measured, it is not immediately obvious whether they reflect structural differences other than the straightforward effect of concentration change.

One feature clearly visible in Figure 1 is the gradual but complete change of the shape of the double peak in the region of 2.0–3.5 Å⁻¹ with changing chemical composition of the solutions. This double peak is a typical structural feature of water and most aqueous solutions, connected to the extended hydrogen-bonded network of water. It is well-known that the shape of the second peak is especially sensitive to the disruption of the hydrogen bonding; e.g., at high temperature the two peaks merge, while at high pressure the second peak sharpens distinctly.²⁹ Moreover, increasing concentrations of dissolved salts visibly change these two peaks, e.g., in the systematic structural studies of AlCl₃³⁰ and alkali halide solutions.²⁴ A

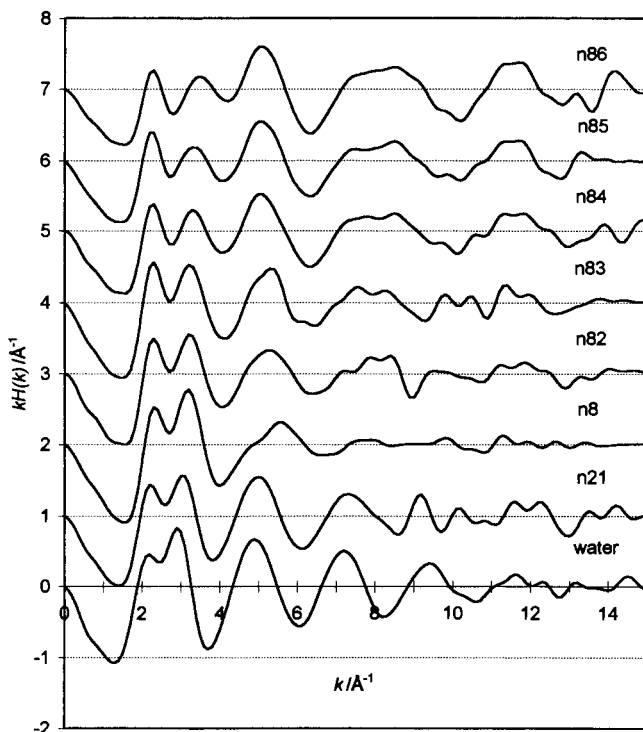


Figure 1. Experimental X-ray structure functions for water, a sodium hydroxide solution, and sodium aluminate solutions. The solutions are as defined in Table 2.

similar effect has also been ascribed to changing cationic radii.²⁴ Of course, other factors may have similar effects because the structure function is a sum of interfering waves, each originating from the different contributions of the component species.

However, there are changes which can be clearly assigned to specific factors in the present series of solutions. Thus, the increasing concentration of aluminum in the solutions has a major effect, causing a substantial decrease of height and a shift in the position of the second peak and also the emergence of the broad fourth and fifth peaks in place of the damping peaks of pure water. This means that the Al-containing structural units in the system strongly influence the original water structure. By contrast, when the samples water, *n21*, and *n8* are compared, it can be seen that changes in sodium hydroxide concentration do not much affect the double peak but (comparing *n8* with water and *n21*), rather, cancel out the waves at $k > 6 \text{ \AA}^{-1}$. This can be due either to interference or to a structural effect, but it certainly occurs in competition with the enhancing effect of Al mentioned above.

Experimental Pair Distribution Functions. The structural features of the solutions can be seen more directly from the pair distribution functions. The experimental pair distribution functions, $g(r)$, were computed from the structure functions according to eq 3, with appropriate cutoff distances (k_{max} values) being applied. The generally accepted data treatment procedure was followed in order to reduce the spurious ripples on the $g(r)$ functions that arise because of the finite truncation of the series. In particular, the pair distributions were back-Fourier transformed to the k -space, while zero was assigned to all $g(r)$ values up to a given r_{min} . The latter limit was determined on the assumption that no interatomic distances can occur in the liquid for all $r < r_{\text{min}}$ and, therefore, any contribution to $g(r)$ has no physical meaning. The values were set to $r_{\text{min}} = 1.5 \text{ \AA}$ for all aluminate solutions, $r_{\text{min}} = 2.0 \text{ \AA}$ for the *n8* solution (pure NaOH) and $r_{\text{min}} = 2.4 \text{ \AA}$ for water. Note that these limits conform to the selection of effective radii for the hypothetical

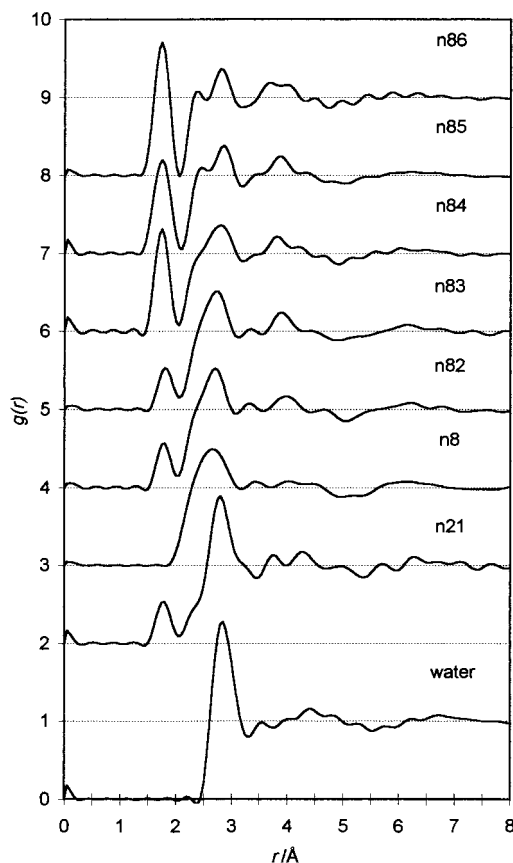


Figure 2. Experimental X-ray pair distribution functions for water, a sodium hydroxide solution, and sodium aluminate solutions. The solutions are as defined in Table 2.

scattering units. The structure functions were then again Fourier transformed to $g(r)$, with the functions obtained shown in Figure 2. It is evident that some of the ripples still remain, albeit to a minor extent. This is the usual residual error of solution X-ray diffractometry. Of significance here is the possible effect of this error on the first peak in the aluminate solutions and thus on the accuracy of the key structural parameters.

Water. The pair distribution function of water is already well-known from the literature. The shape of the present curve is in excellent agreement with published functions.^{28,31} The main peak, at 2.84 \AA , corresponds to hydrogen-bonded first neighbor distances, with an average coordination number of about 3.5 to 4.5 molecules, depending on whether the integration is carried out on half of the main peak (before the maximum) and doubled or whether it is taken to the $g(r)$ minimum, thereby incorporating the asymmetry of the distribution. The usual interpretation of the water structure involves loose, distorted tetrahedra within a 3-dimensional hydrogen-bonded network and is associated with a broad maximum between 4 and 5 \AA , with the main contributions originating from the edges of the tetrahedra.

NaOH Solution. Compared to that of pure water, the pair distribution function of the *n8* solution, (8 M NaOH) shows a broadening of the first peak, with a substantial decrease in height and a significant shift of the peak position down to 2.7 \AA . This feature can be easily explained by taking into account the $\text{Na}^+ - \text{H}_2\text{O}$ first neighbor distance, which is around 2.4 \AA .^{24,32} Thus, the main peak includes contributions of the shorter $\text{Na}^+ - \text{O}$ distances (O being either from an H_2O molecule or an OH^- ion) and the longer $\text{H}_2\text{O} - \text{H}_2\text{O}$ distances.

Aluminate Solutions. The gradual emergence of a shoulder on the left-hand side of the same peak in aluminate solutions

TABLE 2: Approximate Values of the Structural Parameters from a Direct Reading of the Pair Distribution Functions (peak maxima r_1 , r_2 , r_3 , and minima, r_{\min} , in Å), and Coordination Numbers (c_i) Calculated from the Integration to the Peak Maxima ($i < 4$) and to the First Minimum on the $G(r)$ Function ($i = 4$)^a

parameter	peak assignt	water	$n21$	$n8$	$n82$	$n83$	$n84$	$n85$	$n86$
r_1	Al—O		1.80		1.80	1.81	1.75	1.75	1.74
r_2	Na—O		2.35	?	?	2.40	2.40	2.45	2.40
r_3	O—O	2.85	2.80	2.65	2.70	2.75	2.80	2.85	2.85
r_{\min}			3.10	3.15	3.10	3.15	3.20	3.20	3.20
c_1	Al—O		3.9		3.5	2.6	4.1	3.7	4.2
c_2	Na—O		4.5	5.4	4.4	3.8	4.6	5.2	5.2
c_3	O—O	3.2	3.7	5.5	4.9	5.5	6.3	7.1	8.6
c_4	O—O	4.1	4.0	7.5	4.7	5.3	6.9	7.2	9.0

^a Only the predominant contribution is considered for the assignment in column 2. O refers to either OH⁻ or H₂O units.

can also be ascribed to this Na⁺—O contribution. It is interesting to note that while the concentration of sodium is the same in all solutions except $n21$, the shoulder is more pronounced the higher the aluminate concentration. A plausible explanation of this is that a decreasing contribution from the hydrogen bonded H₂O—H₂O distances is observed instead of an increase in the Na⁺—O contribution, leading to a greater separation of the two.

A gradual structural rearrangement can also be observed in the range of longer distances, say, from 3.5 to about 6 Å. It is not possible to assign these changes to one or two pair contributions only. However, the tendency is clear: with increasing aluminate concentration, a broad peak emerges in the range 3.3–4.3 Å, followed by a minimum in the range 4.5–5.5 Å. This longer range structure replaces the broad maximum of pure water, between 4 and 5 Å, and the broad minimum from 5 to 6 Å. This is obviously due to a structural rearrangement, readily explained by the breaking of the longer range structure of bulk water and the development of a more compact, shorter range local order in the more concentrated electrolyte solutions.

This effect can be analyzed quantitatively. The main structural parameters of the experimental $g(r)$ functions, obtained either by direct reading of the functions (maximum and minimum positions and assignment of distances) or by the integration of the area under the peaks (corresponding to coordination numbers) are listed in Table 2. The signs of the charged ions have been neglected for brevity.

Particular care must be taken with two aspects of the interpretation of these parameters. First, there is the well-known “smearing” of the parameters due to the mathematical consequences of the Fourier transformation of structure functions. In essence, there is a convolution of the structure-dependent term with that containing the scattering factors (eq 5 below). Second, the limitations of visible analysis and rough integration must be remembered. The accuracy of estimation regarding the first, well-separated peak positions is ± 0.025 Å, corresponding to the fact that each $g(r)$ was only computed to 0.05 Å units. The other peaks and shoulders cannot be located more accurately than ± 0.05 Å. The coordination number can be estimated to ± 0.5 at best, but may be as poor as ± 1 –2 units for the broader peaks or those resolved from composite ones. The longer the distance, the worse the situation becomes.

The following are worth noting:

(a) The Al—O distance decreases as the concentration of the aluminate ions increases (from 1.80 Å at 1 M Al(OH)₃ to ca. 1.74 Å at 6 M).

(b) The coordination number of the nearest O units around each aluminum is 4, within the limit of the experimental errors. The values for the $n82$ and $n83$ solutions (3.5 and 2.6, respectively) are lower, but this should be regarded with caution as both peaks are rather broad and the first peak is not well resolved.

(c) The position of the Na—O shoulder is unchanged, within the precision of the measurements.

(d) The O—O peak position decreases with the addition of NaOH to water (from 2.85 to 2.65 Å in the $n8$ solution), but this trend is reversed by increasing the aluminate concentration (up to 2.85 Å in the $n86$ solution).

(e) The sodium ions are coordinated by 4.0 to 5.5 O-containing units over the series of aluminate solutions. The highest coordination number, interestingly, is obtained for the pure NaOH solution (5.4) and for those of highest aluminate concentration ($n85$ and $n86$), with the minimum (3.8) exhibited by the $n83$ solution.

(f) If the integrated area corresponding to the Na—O contribution is subtracted from the composite second peak and it is assumed that only O—O scattering contributes to the remainder of the peak, the coordination numbers obtained show a clear tendency to increase with increasing aluminate concentration. This is observed whether the peak maximum (c_3) or the first minimum (c_4) is used as the upper limit of integration. The coordination numbers of water are close to those of the pure solvent in the most dilute ($n21$) solution, but they increase to a value near 9 in the most concentrated solution. There is, therefore, only a relatively slight change of structure in the $n21$ solution but a complete structural rearrangement with increasing concentration, since it is not physically possible to have more than six H₂O molecules coordinated by other H₂O molecules at normal temperatures and pressures at nearest neighbor distances. It is noteworthy that there is hardly enough water in these solutions to satisfy the stoichiometric requirements of such high coordination numbers. The assumption that only O—O type interactions contribute to the right-hand side of the second peak must therefore be dropped and a more complex structural arrangement assumed instead.

Geometric Models of Structure. To understand better the structural features listed above and to determine the structural parameters more precisely, average geometrical models were constructed and tested against the experimental data. The usual procedure is to apply a nonlinear least-squares method (LSQ) in which the theoretical structure functions are calculated with adjustable structural parameters and geometrical rules arising from the models used to compute the nonadjustable parameters. The theoretical structure functions are then compared with the corresponding experimental ones to achieve the best fit, as indicated by the minimum value in

$$R = \frac{\sum_{k=k_{\min}}^{k_{\max}} [kH_{\text{theor}}(k) - kH_{\text{exp}}(k)]^2}{\sum_{k=k_{\min}}^{k_{\max}} k^2 H_{\text{exp}}^2(k)} \quad (4)$$

TABLE 3: Average Weights (as Percentages) of the Contributions of $\alpha\beta$ Type Pairs to the X-ray Structure Functions for the Sodium Hydroxide and Sodium Aluminate Solutions Studied

$\alpha\beta$	<i>n8</i>	<i>n21</i>	<i>n82</i>	<i>n83</i>	<i>m84</i>	<i>n85</i>	<i>n86</i>
Na ⁺ –Na ⁺	2.39	0.38	2.16	2.21	1.94	1.93	1.95
Al–Na ⁺	0.00	0.40	1.40	1.83	2.48	3.10	3.66
Al–Al	0.00	0.11	0.23	0.39	0.80	1.25	1.74
OH [–] –Na ⁺	3.17	1.11	5.03	5.79	6.51	7.42	8.35
OH [–] –Al	0.00	0.58	1.62	2.39	4.15	5.92	7.81
OH [–] –OH [–]	1.07	0.83	2.99	3.87	5.59	7.27	9.12
H ₂ O–Na ⁺	21.87	9.71	17.60	16.60	13.95	12.36	10.93
H ₂ O–Al	0.00	3.87	4.74	5.88	7.94	9.02	9.65
H ₂ O–OH [–]	13.57	12.96	20.33	22.01	24.37	25.50	25.87
H ₂ O–H ₂ O	57.93	70.06	43.90	39.03	32.27	26.23	20.92

The theoretical structure function has its usual form

$$kH_{\text{theor}}(k) = \sum_{\alpha} \sum_{\beta} w_{\alpha\beta}(k) c_{\alpha\beta} j_0(kr_{\alpha\beta}) \exp(-l_{\alpha\beta}^2 k^2/2) - kH_{\text{cont}}(k) \quad (5)$$

where the summation spans each pair of $\alpha\beta$ type contributions, $r_{\alpha\beta}$ is the distance, $l_{\alpha\beta}$ is its root-mean-square deviation (rmsd) value related to the temperature factor, and $c_{\alpha\beta}$ is the frequency factor (coordination number) of the $\alpha\beta$ type contribution. $kH_{\text{cont}}(k)$ denotes the term for those contributions in which the distances are supposed to be randomly distributed. The weight-factor is calculated as

$$w_{\alpha\beta}(k) = \frac{(2 - \delta_{\alpha\beta}) x_{\alpha} x_{\beta} f_{\alpha}(k) f_{\beta}(k)}{\sum_{\alpha} [x_{\alpha} f_{\alpha}(k)]^2} \quad (6)$$

where $\delta_{\alpha\beta}$ is the Kronecker delta.

The average weight of an $\alpha\beta$ type contribution to the structure function is

$$\langle w_{\alpha\beta} \rangle = \frac{\int_{k_{\min}}^{k_{\max}} w_{\alpha\beta}(k) dk}{\int_{k_{\min}}^{k_{\max}} dk} \quad (7)$$

Table 3 summarizes the average weights in percentages, of all $\alpha\beta$ pair contributions to the overall scattering pattern of the studied solutions. Examination of the average weights during the structural analysis is useful in order to decide which pair contributions have a significant effect on the overall scattering pattern and thus which need to be included in the analysis. There are some cases, however, when even the contributions with small weights are of importance. A typical example is the Al–OH contribution, which appears as a well-separated, well-shaped peak in the $g(r)$ function, even for the relatively dilute *n21* solution. The related distance values could thus be accurately determined even though the corresponding average weight was only 0.6%.

The following strategy for the refinement of the structure was adopted. First, a univariate fit was carried out to determine the average distance values for Al–OH pair distributions. The decrease in LSQ sum and a graphical goodness-of-fit for the relevant peak on the experimental $g(r)$ function were monitored simultaneously. The same procedure was applied to obtain the corresponding $l_{\alpha\beta}$ and $c_{\alpha\beta}$ values. Once these parameters were determined and the existence of four coordinate Al atoms consequently established, the contributions of OH–OH pairs within the Al(OH)₄[–] tetrahedra were determined from geo-

metrical constraints. Next, the contributions of the monomer structural units were subtracted from the experimental $kH(k)$ and the Na–O parameters determined approximately. Finally, an attempt was made to determine the parameters for the bulk water in the system.

Once a rough estimate for each main parameter had been obtained, a systematic refinement was performed by testing the following species in the model.

(1) Aluminate ions in monomeric form, corresponding to the formula Al(OH)₄[–]. A regular tetrahedral shape was assumed and the OH–OH distances and coordination numbers were computed accordingly.

(2) Aluminate ions in dimeric form, corresponding to the formula Al₂O(OH)₇[–].⁹ Two regular tetrahedra were assumed with a shared common O atom at one of their vertexes. All distances and coordination numbers were computed from the geometrical constraints. The assumption of binding between the two tetrahedra by two hydrogen bonds between OH units from each tetrahedron (in addition to the Al–O–Al linkage) was also included in the model. Justification for these postulates is given later.

(3) The hydration structure of the aluminate ions was characterized by Al–H₂O pairs, with the relevant distances and coordination numbers taken as free parameters.

(4) Hydrated sodium ions were characterized by structural parameters of Na–H₂O contributions. No regular geometry was assumed.

(5) Sodium hydroxide contact ion pairs were considered, with the number of pairing distances restricted by the NaOH excess over the concentration of aluminate ions. Distances and rmsd values of the Na–OH pairs were set equal to those for Na–H₂O and were refined simultaneously.

(6) Sodium aluminate contact ion pairs were assumed to have a sodium ion in touch with three OH groups, i.e., on the face of the aluminate tetrahedron. Correspondingly, only one Al–Na distance was included in the model.

(7) The structure around the hydrated hydroxide ions was considered to be identical to the first neighbor distance of coordinated water molecules in bulk water. Distances and coordination numbers were then adjusted during the fitting procedure.

(8) The remaining water structure was described by three different contributions, with characteristic distances estimated initially from the location of the third, fourth, and fifth maxima in the $g(r)$ functions. Distances and coordination numbers were then adjusted. The term “remaining water structure” in this paper refers to bulk water and/or to structural contributions from the water–water distances around hydrated ions or hydrated ion pairs.

(9) Rmsd values were adjusted to take account of the Al–OH contributions and for all others with relatively high average weights. In all other cases rmsd values were fixed, and set equal to an approximate value chosen from the literature.³²

(10) The “continuous” part of the structure function was omitted from the structural analysis, as it is irrelevant to the local order of current interest.

During the analysis, the model comprised an appropriate mixture of the above elements. Initially, an assumption of fully hydrated ion pairs merged in the “remaining water structure” was adopted, without accounting for any ion pair formation. This model was then developed by dropping the assumption of complete hydration to consider the system with ion pairs. Finally, a compact structure in which all the aluminate ions were regarded as forming contact ion pairs with sodium and these

TABLE 4: Structural Parameters Obtained from Least-Squares Fitting of the Experimental Data by Theoretical Structure Functions, Using Average Geometrical Models^a

	parameter	<i>n21</i>	<i>n82</i>	<i>n83</i>	<i>n84</i>	<i>n85</i>	<i>n86</i>
Al(OH) ₄ monomer	<i>r</i> _{Al-OH}	1.796	1.788	1.851	1.751	1.756	1.744
	<i>l</i> _{Al-OH}	0.083	0.073	0.107	0.072	0.128	0.083
	<i>c</i> _{Al-OH}	4.189	3.950	3.360	4.144	4.266	4.300
	<i>r</i> _{OH-OH}	2.934	2.920	2.915	2.860	2.867	2.849
	<i>l</i> _{OH-OH}	0.160	0.160	0.160	0.160	0.138	0.140
	<i>c</i> _{OH-OH}	6*	6*	6*	6*	6*	6*
Na ⁺ -Al(OH) ₄ ion pair	<i>r</i> _{Na-O}		2.363	2.411	2.394	2.456	2.387
	<i>l</i> _{Na-O}		0.127	0.144	0.165	0.113	0.102
	<i>c</i> _{Na-O}		1.505	1.649	2.007	2.256	2.473
	<i>r</i> _{Al-Na}			2.386	2.367	2.369	2.363
	<i>l</i> _{Al-Na}			0.15	0.15	0.15	0.15
	<i>c</i> _{Al-Na}			1*	1*	1*	1*
Na ⁺ -H ₂ O hydrate	<i>r</i> _{Na-H₂O}	2.356	2.363	2.411	2.394	2.456	2.387
	<i>l</i> _{Na-H₂O}	0.128	0.127	0.144	0.165	0.113	0.102
	<i>c</i> _{Na-H₂O}	3.690	3.694	2.500	2.419	2.078	1.102
OH ⁻ -H ₂ O hydrate	<i>r</i> _{OH⁻-H₂O}		2.743	2.763	2.755	2.851	2.800
	<i>l</i> _{OH⁻-H₂O}		0.138	0.157	0.170	0.154	0.169
	<i>c</i> _{OH⁻-H₂O}		0.000	1.802	1.207	1.328	1.143
Al-H ₂ O hydrate	<i>r</i> _{Al-H₂O}		4.300	4.200	4.300	4.282	4.000
	<i>l</i> _{Al-H₂O}		0.271	0.271	0.271	0.249	0.250
	<i>c</i> _{Al-H₂O}		4.565	4.156	4.561	5.659	4.954
H ₂ O-H ₂ O bulk	<i>r</i> _{H₂O-H₂O}	2.795	2.743	2.763	2.842	2.851	2.838
	<i>l</i> _{H₂O-H₂O}	0.143	0.139	0.157	0.170	0.154	0.171
	<i>c</i> _{H₂O-H₂O}	3.460	3.836	3.047	3.456	3.561	3.456
	<i>r</i> _{H₂O-H₂O}	3.272	3.343	3.353	3.359	3.346	3.248
	<i>l</i> _{H₂O-H₂O}	0.179	0.223	0.258	0.258	0.194	0.227
	<i>c</i> _{H₂O-H₂O}	2.752	4.369	5.198	4.829	4.669	4.338
	<i>r</i> _{H₂O-H₂O}	3.773	3.947	3.901	3.857	3.823	3.678
	<i>l</i> _{H₂O-H₂O}	0.185	0.265	0.255	0.209	0.209	0.224
	<i>c</i> _{H₂O-H₂O}	4.319	4.727	5.076	5.729	6.737	4.732

^a The distances, (*r*_{*αβ*}), the rmsd deviations (*l*_{*αβ*}) in Å, and the coordination numbers (*c*_{*αβ*}) are given. Asterisks indicate that the parameters were fixed during the fitting procedure or calculated from geometrical constraints.

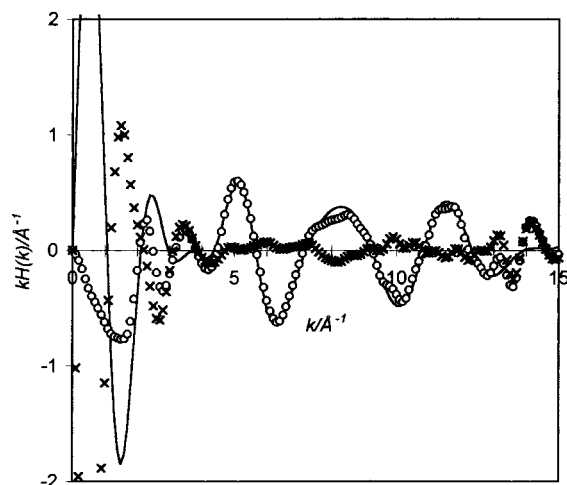


Figure 3. Result of the LSQ fitting procedure for the *n86* sodium aluminate solution at the structure function level, showing the experimental X-ray structure function (circles), the best fitting theoretical structure function (full line), and the difference (crosses).

“compact” structural units were hydrated by the remaining water molecules and/or form contact ion pairs with hydroxide ions was assumed. In the last case, no allowance was made for separate hydrated ions in the solution. The structural parameters obtained from models which give the best fit to the experimental data are listed in Table 4.

The agreement between the best fitting theoretical structure functions and the corresponding experimental structure function for the *n86* solution is shown in Figure 3. Omission of the continuous part from the fitting procedure largely influences the range $k < 4 \text{ \AA}^{-1}$, but the agreement is also very good with higher *k* values.

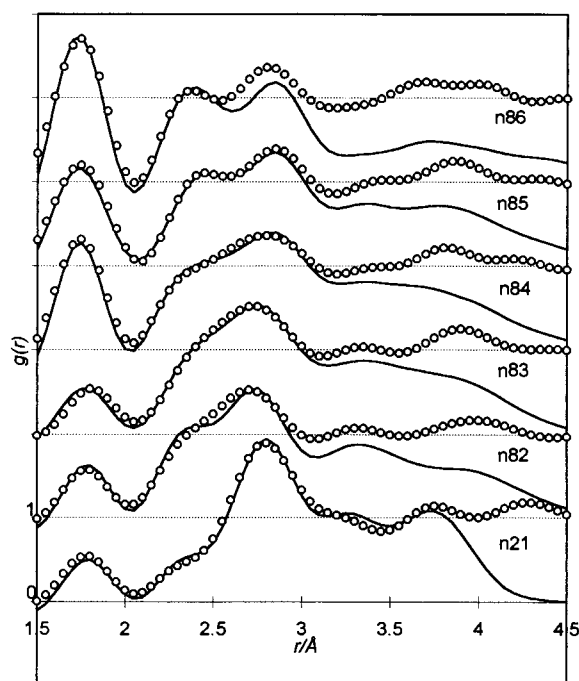


Figure 4. Experimental X-ray pair distribution functions (circles) and best-fitting theoretical simulations (full lines), based on the average geometrical model assumptions for the highly concentrated sodium aluminate solutions.

The agreement between the theoretical and experimental pair distribution functions for the aluminate solutions is shown in Figure 4 over the range from 1.5 to 4.5 Å. Excellent fits are achieved except at longer distances where a uniform distribution of the diffraction distances gradually predominates which was,

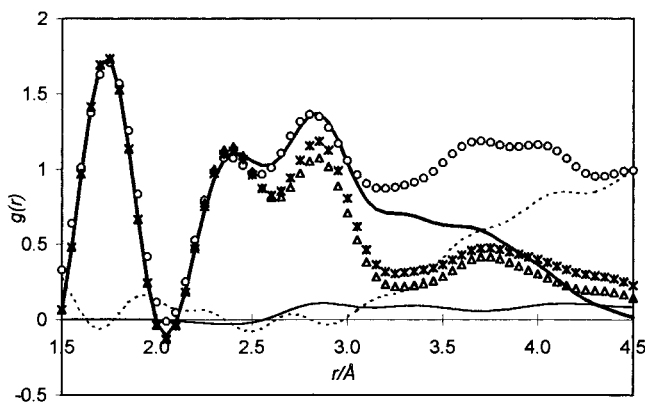


Figure 5. Comparison of the X-ray pair distribution functions, computed from the various geometrical models for the most concentrated sodium aluminate solution *n*86. The complete model (thick line), a model including $\text{Al}(\text{OH})_4^-$ monomers plus $\text{Na}^+ - \text{Al}(\text{OH})_4^-$ ion pairs (triangles), and a model including $\text{Al}_2\text{O}(\text{OH})_6^-$ dimers plus $\text{Na}^+ - \text{Al}(\text{OH})_4^-$ ion pairs (asterisks) are shown. Experimental X-ray pair distribution functions are represented by circles, the difference between the contributions of the dimers and the monomers by a thin line, and the remainder of the experimental pair distribution function after the subtraction of the curve for the complete model by a dashed line.

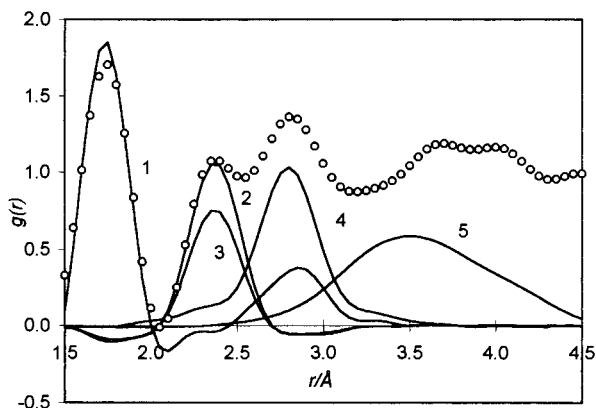


Figure 6. Details of the contributions to the theoretical X-ray pair distribution function, computed for the most concentrated sodium aluminate solution (*n*86). Contributions arising from the $\text{Al}(\text{OH})_4^-$ monomeric unit (1), $\text{Na}^+ - \text{Al}(\text{OH})_4^-$ ion pairs (2), $\text{Na}^+ - \text{OH}^-$ ion pairs and $\text{Na}^+ - \text{H}_2\text{O}$ contributions from hydrating water molecules (3), $\text{OH}^- - \text{H}_2\text{O}$ and $\text{H}_2\text{O} - \text{H}_2\text{O}$ first neighbor contributions (4), and further $\text{H}_2\text{O} - \text{H}_2\text{O}$ contributions from longer distances (5) are shown.

in turn, omitted from the fitting procedure. More detail of the structural contributions is given in Figures 5 and 6, which show the residual curve (Figure 5, dashed line) and the separate contributions of various assumptions (Figure 6, numbered curves), in the development of the model.

Discussion

The Local Structure around Aluminum. There is ample evidence in the literature that the distance between aluminum(III) and coordinated oxygen atoms depends on the coordination geometry of the aluminum.^{29,33–39} Thus, in solution, the Al^{3+} ions were reported to be completely hydrated by six water molecules in an octahedral configuration. The average $\text{Al}^{3+} - \text{OH}_2$ distance was found to be 1.90 and 1.89 Å in 1 and 2 M aluminum chloride solutions, respectively,³⁰ and 1.90 and 1.87 Å in 0.5 and 3.5 M aluminum nitrate solutions, respectively.^{33,34} The slight drop of distance values with increasing concentration is comparable with the experimental error.

In the solid state, whenever aluminum atoms are found to be six coordinate, the observed Al–O distances are also close to

1.90 Å. Thus, in crystal structures of $[\text{Al}_2(\text{OH})_2(\text{H}_2\text{O})_8](\text{SO}_4)_2 \cdot 2\text{H}_2\text{O}$ and $[\text{Al}_2(\text{OH})_2(\text{H}_2\text{O})_8](\text{SeO}_4)_2 \cdot 2\text{H}_2\text{O}$ the complexes exist as $[\text{Al}_2(\text{OH})_2(\text{H}_2\text{O})_8]^{4+}$ units with Al–O distances from 1.87 to 1.91 Å in the AlO_6 octahedra³⁵ and in $\text{Na}_5[\text{Al}(\text{OH})_6](\text{OH})_2$ the monomeric $[\text{Al}(\text{OH})_6]^{3-}$ anions have Al–O distances of about 1.93 Å.³⁶ In the $\text{Na}_9[\text{Al}(\text{OH})_6]_2(\text{OH})_3 \cdot 6\text{H}_2\text{O}$ crystal, the Al occurs as monomeric octahedral anion $[\text{Al}(\text{OH})_6]^{3-}$ with Al–O distances varying between 1.89 and 2.00 Å.^{37,38} It is worth noting that some of the distances are longer in the latter crystal than in the others. These variations can perhaps depend on the nature of the coordinating O-species (i.e., OH instead of OH_2), but it seems that this effect is never very large.

As far as tetrahedrally coordinate aluminum is concerned, no previous measurements appear to have been made in solution. However, abundant data are available for aluminate species with four-coordinate aluminum complexes in the solid state and they demonstrate a significant shortening, by about 0.15 Å, in the Al–O distances compared to those in octahedral complexes. In particular, in a $\text{Na}_2[\text{Al}(\text{OH})_4]\text{Cl}$ crystal the four Al–O(H) distances are 1.756 Å long.³⁹ Again, the nature of the coordinating group does not have a large effect: the Na_5AlO_4 crystal consists of isolated AlO_4 tetrahedra⁴⁰ with distances from 1.761 to 1.789 Å.

A distinction worth being made occurs between bridging Al–O(Al) and terminal Al–O(H) distances in the crystalline phase. Potassium aluminate crystals of composition $\text{K}_2[\text{Al}_2\text{O}(\text{OH})_6]$ that contain $[(\text{OH})_3\text{AlOAl}(\text{OH})_3]^{2-}$ dimer structures, i.e., are built up from two AlO_4 tetrahedra sharing an oxygen,⁴¹ have the four distances within the tetrahedron as 1.73, 1.75, 1.76, and 1.78 Å, with 1.73 Å being the Al–O(Al) distance. Similarly, in a $\text{Na}_2[\text{Al}_2\text{O}_3(\text{OH})_2] \cdot 1.5\text{H}_2\text{O}$ crystal, the three Al–O(Al) distances were found to be 1.729, 1.745, and 1.763 Å, compared with that for Al–O(H) at 1.789 Å.⁴² The bridging Al–O(Al) distances are also found to be shorter in crystals where the structure is built from an extended polymeric network. In its triclinic form, $\text{Na}_7\text{Al}_3\text{O}_8$ consists of infinite chains of Al_6O_{16} rings linked by oxygen bridges and $\text{Na}_{17}\text{Al}_5\text{O}_{16}$ consists of discrete Al_5O_{16} chains of corner-sharing AlO_4 tetrahedra;^{43,44} the Al–O distances are in the range of 1.71–1.80 Å.

The listed literature values show that in the crystalline phase, the change of octahedral coordination to tetrahedral has the greatest effect on the Al–O distances (a shortening of 0.15 Å). Less significant is the difference between bridging and terminal Al–O distances (at about 0.03–0.05 Å), while the chemical nature of the coordinating species has the least effect. It is also important to observe that the distances in octahedral complexes in the liquid phase are in good agreement with those in the crystalline phase. It is therefore reasonable to expect a similar agreement for four coordinate aluminum in the solution and solid states as well.

In the present study, the LSQ fitting procedure leads to two conclusions. First, the refined average $r_{\text{Al}-\text{OH}}$ distances shorten with increasing aluminate concentration, as shown in Figure 7. It is important to note that unlike in AlCl_3 and $\text{Al}(\text{NO}_3)_3$ solutions, this is a significant change and therefore is indicative of a speciation change in solution. A linear regression analysis for the equation

$$r_{\text{Al}-\text{OH}} = mx + n \quad (8)$$

where x is the aluminate concentration expressed as $\text{Al}(\text{OH})_3$ in M, yields $m = -0.011 \text{ Å mol}^{-1} \text{ dm}^3$ and $n = 1.8 \text{ Å}$.

Second, the coordination number of the O-containing scattering units around the Al atoms in all of the present aluminate solution is four, within the limit of experimental error. It is

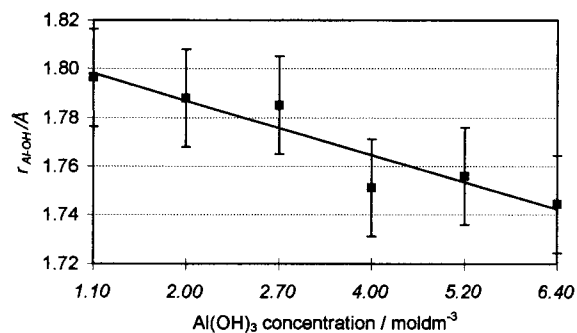


Figure 7. Average values of the distances of OH groups from the Al atoms within an aluminate unit as a function of aluminate concentration in highly concentrated sodium aluminate solutions. The distance values were determined by a LSQ fitting procedure of hypothetical structure functions to the experimental ones, obtained from X-ray diffraction. The error bars indicate the estimated errors of determination. The straight line was determined by linear regression analysis.

interesting to note that the LSQ fit produced coordination values closer to four than were estimated from the direct reading of parameters from the pair distribution functions. The accurate values of distances, together with the coordination values and the literature information establish that the basic structural geometry of the aluminate ions in all our solutions is tetrahedral.

An attempt was also made to describe the structure of the (more concentrated) solutions by including a dimeric species $[(\text{HO})_3\text{AlOAl}(\text{OH})_3]$ which has two tetrahedrally coordinated aluminum atoms with an O atom shared at a common vertex (listed as model 2 in the previous section). This structure has been proposed by Moolenaar et al.⁹ on the basis of their Raman studies of aluminate solutions and has also been observed in the solid state.^{39,42} The geometry of the latter studies was adopted in the present modeling. Unfortunately, the contributions to the pair distribution function that might be due to any dimeric units are not sufficiently different from those of the monomeric species to draw any positive conclusion (see Figure 5). Given the accuracy of the distances, it proved impossible to determine the percentage to which any dimeric species might be present in solution, either from the average values of the distances, or from a direct fitting of the various model combinations to the experimental data.

Hydration Structure of the Aluminate Ion and the First Neighbor Oxygen–Oxygen Distances. Adding the approximate effective radii of Al, OH, and H₂O gives an Al–OH₂ distance of between 4.0 and 4.4 Å for hydrated aluminate species. The distance depends slightly on the location and orientation of the hydrating water molecule. For trivalent, hydrated Al³⁺ ions, a strong tendency to form a stable and highly symmetrical second hydration layer with hydrogen bonds significantly shorter than those present in pure water has been observed.^{30,34} This was explained in terms of the strong coulombic field of Al³⁺ which strongly polarizes its first neighbor molecules. In contrast, as the Al(OH)₄⁻ is both an anion and much larger, it seems likely to have only a very loosely bound hydration shell like perchlorate, sulfate, or iodide.³² This fact, and the complexity of the entire structure in the range up to the expected Al–OH₂ distance, have made the determination of the aluminate hydration parameters quite uncertain. Although refinement of the distance and coordination numbers was attempted and the resulting values seem to be acceptable (see Table 4), it would be unwise to draw any firm conclusions from them.

Coordination Structure of the Sodium Ion: Hydration and Contact Ion Pair Formation. The hydration structure of

sodium ions in solution has been intensively investigated by direct structural methods³² but with a surprisingly scattered range of results. The hydration numbers that have been reported usually vary between 4 and 6, with Na–O distances between 2.4 and 2.5 Å. Computer simulation studies have explained these variations by invoking the existence of relatively weak forces between sodium and water, which result in a loss of regular symmetry in the first hydration shell.⁴⁵

Sodium aluminate crystal structures also demonstrate a versatility in sodium coordination. In the Na₉[Al(OH)₆]₂(OH)₃·6H₂O crystal^{35,38} all Na⁺ ions are octahedrally coordinated by water molecules and OH⁻ ions, with Na–O distances varying from 2.33 to 2.58 Å. In Na₅[Al(OH)₆](OH)₂, an octahedral coordination is also reported.³⁶ In the Na₂[Al(OH)₄]Cl crystal the sodium ion is six coordinate, the Na–O distance is 2.435 Å, and the hydroxide O is shared with the aluminum, forming a contact ion pair.³⁹ In the Na₂[Al₂O₃(OH)₂]0.1,5H₂O crystal sodium is again octahedrally coordinated.⁴² In Na₇Al₃O₈ and in Na₁₇Al₅O₁₆ the coordination of sodium is rather complex, being either four or five coordinated and with the Na–O distance varying between 2.22 and 2.80 Å, while in the Na₅-AlO₄ crystal the sodium is four coordinated and the Na–O distances vary between 2.21 and 2.55 Å.^{39,43}

The present results regarding the coordination structure of the sodium ions in solution conform with the above observations. The Na–O distances are in good agreement with earlier liquid phase studies, with the refined values around the lower limit of those previously reported (2.40 Å). The average coordination number of Na⁺ in the most highly concentrated NaOH solution (*n*8) is 5.4. This represents a significantly lower degree of symmetry than would be the case in a truly octahedral structure.

The coordination state of the sodium ion in the sodium aluminate solutions is more complicated. In the most dilute solutions (*n*21 and *n*82) the hydration number of sodium is already significantly less than in the pure sodium hydroxide solution, with an average coordination number of 3.7. Interestingly, this decreases further as the aluminate concentration increases, down to just one water molecule in the vicinity of Na⁺ ion at an aluminate concentration of 6 M. This is an obvious consequence of the shortage of bulk water. On the other hand, due to the formation of contact ion pairs in these solutions, the O atoms of the aluminate ions participate increasingly in the sodium ion coordination, with the number increasing from 1.5 in the *n*82 solution to 2.47 in the *n*86 solution. If it is assumed that the sodium aluminate ion pair comprises a sodium ion in contact with one face of the aluminate tetrahedron (i.e., it “sits” in the cavity formed by the three OH groups), the distance between aluminum and sodium can be calculated from the geometry of the tetrahedron and the radius of the sodium ion. The result is very similar to the Na–O distances usually found between a sodium ion and a water molecule or OH group in contact with it (3.36–3.38 Å). Adding the number of hydrating water molecules to the OH groups coordinating the aluminum ion gives a coordination number around 5.5, about the same as in pure sodium hydroxide solution. This explains why the coordination number of sodium at high concentrations of aluminate is similar to those in pure sodium hydroxide solution, as was determined by the direct integration described above.

A rough estimate of the percentage of sodium (and aluminate) ions involved in the ion pairs can be made by assuming that in each contact ion pair one sodium ion touches one face of an aluminate tetrahedron. The possible maximum number of OH⁻ groups in contact is then 3. The observed average $c_{\text{Na-O}}$ values

suggest that, on this basis, about 50% of aluminate ions are involved in ion pairs in the *n*82 solution while the ratio is above 80% in the *n*86 case. These percentages are, of course, only rough estimates. Since sharing of sodium between OH groups is expected and would cause the extent of ion pair formation to be underestimated, there is some probability that a much higher percentage of contact ion pairs occurs, perhaps up to 100%.

Structural Changes in Bulk Water. An assumption usually made in the structural analysis of dilute solutions is that water which is not directly coordinated to a solute species may be treated as bulk water and the experimental structure function of pure water can be simply subtracted from that of the solution. In these cases, a weighting factor is calculated from the stoichiometric ratio of water. This approximation is, however, not valid with the present solutions except, perhaps, *n*21. This makes any attempt to characterize quantitatively the structure of the bulk or, more precisely, of the remaining water, rather difficult. The only reliable statement that can be made is that the original structure of the water is largely disrupted.

An attempt was made to describe the remaining water–water contributions using three terms. The results of this analysis clearly show that drastic changes in the water structure have occurred compared with pure water. One interesting observation is that, relative to pure water, the first neighbor O–O distances are shortened remarkably, even in the more dilute solutions. A gradual increase is also observed with increasing aluminate concentration, up to 2.84 Å, which coincides with the average H₂O–H₂O distance in pure water. It is worth noting that significantly shorter hydrogen bonded water–water distances have also been observed in AlCl₃ and Al(NO₃)₃ solutions. It has been established that nearest neighbor H₂O molecules participate in building a pronounced, well-ordered, second hydration shell around the Al³⁺ ions. This phenomenon is explained by the strong coulombic field of the Al³⁺ which polarizes the first neighboring water molecules and increases the attractive interaction between the first and second hydration sheaths.⁴⁶ This, however, cannot be true of the negatively charged aluminate ion and its neighbors. Nevertheless, the free hydroxide ions can interact with the neighboring water molecules (by hydrogen bonding) more strongly than with the other water molecules. Consequently shorter O–O distances can occur. This corresponds to the number of water molecules in the bulk decreasing with increasing solute concentration and hence less solvent to hydrate the OH[−] ions, causing the average first neighbor distance to increase.

The next two contributions that are assigned to the H₂O–H₂O pairs have their average distances around 3.3 and 3.8 Å, with coordination numbers of 4 to 5, except for the *n*21 solutions which have much lower values. If sodium had an octahedral hydrated structure, the O–O distances at the edge would be 3.4 Å, whereas if the structure was tetrahedral it would be 3.9 Å. These average distances are in good agreement with both results of refinement. It is worth remembering that distances at the edge of tetrahedra formed by water molecules around an OH[−] ion or a water molecule would result in an average O–O value of 4.5–4.6 Å, which is much larger than the ones obtained above.

Summary and Conclusions

As a result of the progressive fitting procedure described above, the best fitted model for the most dilute *n*21 solution includes only Al(OH)₄ monomers, hydrated sodium ions, and bulk water. The hydration structure of the aluminate ion could not be adequately described due to the low weight of Al–OH₂

pair contributions. For the same reason and because of the difficulty in distinguishing between OH[−] and H₂O, the hydration structure of the OH[−] ions could also not be determined. No direct evidence was found for the formation of sodium aluminate contact ion pair formation. The relatively low coordination number in the sodium hydration shell and the shortened value of the first neighbor H₂O–H₂O distances give an indication of the influence of the aluminate ion on their structures.

At the other extreme, in the most concentrated *n*86 solution, there is hardly enough water to completely hydrate any of the ions in solution. The existence of contact ion pairs is thus ensured by simple stoichiometric and packing constraints. For these concentrated solutions, the ions are partly hydrated and partly in contact with each other. The shortening of the H₂O–H₂O (or OH[−]–H₂O) distances compared with the typical first neighbor distances in pure water points to an ordering effect attributable to the coulombic interactions of the ions. The ions of opposite charge form contact ion pairs and these species share the few water molecules in solution between them.

In summary, the speciation in highly concentrated alkaline solutions is dominated by an aluminate ion that is four coordinate and has tetrahedral symmetry. Significant concentrations of species with higher (octahedral) or lower degrees of symmetry (e.g., AlO₂ units) can be excluded. The shortening in the Al–OH distances in solutions with increasing aluminate concentration is in accord with the crystallographic data of solid aluminates in which an O is shared by two Al ions and is thus consistent with the hypothesis by Moolenaar et al.⁹ that an Al₂O(OH)₆^{2−} dimer may coexist with the Al(OH)₄[−] monomers. More importantly, the refinement of our models shows that in dilute solutions (*n*21 and, to some extent, *n*82), hydrated forms of the cations are present. At very high concentrations, however, all ions tend to be involved in contact ion pairs which share the available water molecules. In the intermediate concentration range the analysis of the X-ray data becomes more difficult, probably because a mixture of these two extreme cases occurs.

Acknowledgment. This work was supported by the Australian Department of Industry, Science & Tourism through its Bilateral Science & Technology Program. Partial funding was also provided by an Australian Research Council Collaborative Grant (The Chemical Speciation of Synthetic Bayer Liquors) with the Australian Minerals Industry Research Association through its Project P380B. Dr. F. H. Kármán (CRIC, Budapest) is thanked for technical assistance.

References and Notes

- Hind, A. R.; Bhargava, S. K.; Nunes, M. D.; Grocott, S. C. *Chem. Aust.* **1997**, 22, 36–39.
- Konenkova, T. Y. *J. Appl. Chem. (U.S.S.R.)* **1976**, 49, 2214.
- Plumb, R. C., Jr.; Swaine, J. W. *J. Phys. Chem.* **1964**, 68, 2057.
- Berecz, E.; Szita, L. Second Int. Symp. ICSOBA, Budapest, 1969; *Proceedings* **1971**, 3, 89.
- Szabó, Z. G.; Rózsahégyi-Pálfalvi, M.; Orbán, M. *Acta Chim. Acad. Sci. Hung.* **1978**, 97, 327.
- Diakonov, I.; Pokrovski, G.; Schott, J.; Castet, S.; Gout, R. *Geochim. Cosmochim. Acta* **1996**, 60, 197.
- Arlyuk, B. I.; Mironov, E. I.; Kirillova, T. A. *Sov. J. Non-Ferrous Met.* **1978**, 19, 45.
- O'Reilly, D. E. *J. Chem. Phys.* **1960**, 32, 1007.
- Moolenaar, R. J.; Evans, J. C.; McKeever, L. D. *J. Phys. Chem.* **1970**, 74, 3629.
- Dovbysh, N. G.; Volokhov, Y. A.; Lebedev, V. B.; Sizyakov, V. M.; Mironov, V. E. *J. Struct. Chem. (U.S.S.R.)* **1981**, 22, 137.
- Akitt, J. W.; Gessner, W.; Weinberger, M. *Magn. Reson. Chem.* **1988**, 26, 1047.
- Chen, N.; Liu, M. X.; Yang, J.-Z. *Chin. J. Met. Sci. Technol.* **1992**, 8, 135.

- (13) Bradley, S. M.; Hanna, J. V. *J. Chem. Soc., Chem. Commun.* **1993**, 1249.
- (14) Tyurin, Y. N.; Badich, V. D. *Sb. Khim. Tekhnol. Glinozema, Novosibirsk, Nauka* **1971**, 339.
- (15) Sipos, P.; May, P. M.; Hefter, G. T.; Kron, I. *J. Chem. Soc., Chem. Commun.* **1994**, 2355.
- (16) Carreira, L. A.; Maroni, V. A.; Swaine, J. W.; Plumb, R. C. *J. Chem. Phys.* **1966**, *45*, 2216.
- (17) Pavlov, L. N.; Eremin, N. I.; Konenkova, T. Y.; Mironov, V. E. *Tsvet. Metall.* **1969**, *42*, 56.
- (18) Wajand, J.; Szabó, Z. G.; Ruff, I.; Burger, K. *Magy. Kém. Foly.* **1980**, *86*, 339.
- (19) Myund, L. A.; Sizyakov, V. M.; Khripun, M. K.; Makarov, A. A. *Russ. J. Gen. Chem.* **1995**, *65*, 826.
- (20) Eremin, N. I.; Volokhov, Y. A.; Mironov, V. E. *Russ. Chem. Rev.* **1974**, *43*, 92.
- (21) Zámbo, J. *Light Met.* **1986**, 199.
- (22) Sipos, P.; Hefter, G. T.; May, P. M. *Aust. J. Chem.* **1998**, *51*, 445.
- (23) Sipos, P.; Hefter, G. T.; May, P. M. *Talanta* **1997**, *44*, 617–620.
- (24) Pálinkás, G.; Radnai, T.; Hajdu, F. *Z. Naturforsch.* **1980**, *35a*, 107.
- (25) *International Tables for X-ray Crystallography*; The Kynoch Press: 1974; Vol. 4., p 99.
- (26) Narten, A. H. *J. Chem. Phys.* **1979**, *70*, 299.
- (27) Pálinkás, G.; Radnai, T. *Acta Crystallogr.* **1976**, *A32*, 666.
- (28) Hajdu, F. *Acta Crystallogr.* **1972**, *A28*, 250.
- (29) Radnai, T.; Ohtaki, H. *Mol. Phys.* **1996**, *87*, 103.
- (30) Caminiti, R.; Licheri, G.; Piccaluga, G.; Pinna, G.; Radnai, T. *J. Chem. Phys.* **1979**, *71*, 2473.
- (31) Narten, A. H.; Levy, H. A. *J. Chem. Phys.* **1971**, *55*, 2263.
- (32) Ohtaki, H.; Radnai, T. *Chem. Rev.* **1993**, *93*, 1157.
- (33) Bol, W.; Welzen, T. *Chem. Phys. Lett.* **1977**, *49*, 189.
- (34) Caminiti, R.; Radnai, T. *Z. Naturforsch.* **1980**, *35a*, 1368.
- (35) Johansson, G. *Acta Chem. Scand.* **1962**, *16*, 403.
- (36) Weinberger, M.; Gessner, W.; Schneider, M. *Z. Kristallogr.* **1997**, *212*, 236.
- (37) Zabel, V.; Schneider, M.; Weinberger, M.; Gessner, W. *Acta Crystallogr.* **1996**, *C52*, 747.
- (38) Weinberger, M.; Schneider, M.; Zabel, V.; Gessner, W. *Z. Anorg. Allg. Chem.* **1996**, *622*, 1799.
- (39) Weinberger, M.; Schneider, M.; Müller, D.; Gessner, W.; Reck, G. *Z. Anorg. Allg. Chem.* **1994**, *620*, 771.
- (40) Barker, M. G.; Gadd, P. G.; Begley, M. J. *J. Chem. Soc., Dalton Trans.* **1984**, 1139.
- (41) Johansson, G. *Acta Chem. Scand.* **1966**, *20*, 505.
- (42) Weinberger, M.; Schneider, M.; Müller, D.; and Gessner, W. *Z. Anorg. Allg. Chem.* **1995**, *621*, 679.
- (43) Barker, M. G.; Gadd, P. G.; Begley, M. J. *J. Chem. Soc., Chem. Commun.* **1981**, 379.
- (44) Barker, M. G.; Gadd, P. G.; Wallwork, S. C. *J. Chem. Soc., Chem. Commun.* **1982**, 516.
- (45) Jancsó, G.; Heinzinger, K.; Bopp, P. A. *Z. Naturforsch.* **1985**, *40a*, 1235–1238.
- (46) Mayer, I.; Lukovits, I.; Radnai, T. *Chem. Phys. Lett.* **1992**, *188*, 595.